Food Science WILEY

Palm-based cellulose nanofiber isolated from mechano-chemical processing as sustainable rheological modifier in reduced fat mayonnaise

Zu Jia Lee[1] | Shi-Cheng Tong[1] | Teck-Kim Tang[3] | Yee-Ying Lee[1,2]

[1]School of Science, Monash University Malaysia, Bandar Sunway, Selangor, Malaysia

[2]Monash Industry Palm Oil Research and Education Platform, Monash University Malaysia, Bandar Sunway, Selangor, Malaysia

[3]Institute of Bioscience, Universiti Putra Malaysia, Serdang, Selangor, Malaysia

Correspondence
Yee-Ying Lee, School of Science, Monash University Malaysia, 47500 Bandar Sunway Selangor, Malaysia.
Email: lee.yeeying@monash.edu

Funding information
School of Science, Monash University Malaysia

Abstract: Reducing fat intake from our daily diet serves to be an effective way to combat the rising obesity issue worldwide. Hence, reducing fat content in mayonnaise, a high fat food product, is one of the primary trends in the food industry. To date, research on the use of nanocellulose, a new and emerging form of fat mimetic, in mayonnaise formulation remains limited. This study sets out to formulate reduced fat 5%, 15%, and 30% mayonnaise using varying concentration of nanocellulose synthesized from palm pressed fiber followed by a 20-day stability study. Nanocellulose was synthesized with particle size of 106.0 ± 18.7 nm and zeta potential of -72.5 ± 2.26 mV. It was used as fat mimetic in mayonnaise. Rheological analysis conducted showed that incorporation of nanocellulose into reduced fat mayonnaise formulation was able to counteract the loss of viscosity in mayonnaise caused by fat content reduction. This finding was further supported by the smaller oil droplets that are closely packed in reduced fat mayonnaise formulation when viewed under light microscope. Nonetheless, significant oil droplet coalescence was found in reduced fat mayonnaise formulations during storage period which could lead to loss of viscosity. Taken together, these findings suggest that CNF was able to act as fat mimetic upon formulation of mayonnaise but the same cannot be said during long term storage of mayonnaise.

KEYWORDS
fat mimetic, mayonnaise, nanocellulose, reduced fat, stability

Practical Application: We successfully isolated nanocellulose from palm biomass (palm pressed fiber) using green approach and used it as a fat replacer for preparation of 5%, 15%, and 30% reduced fat mayonnaise. A computation study revealed a strong binding affinity of the nanocellulose on the lipase active site essential to inhibit the digestion of fats and oils. Therefore, nanocellulose demonstrated a huge potential to be used as not only as fat replacer but also rheological modifier for the development of reduced fat or vegan foods.

1 | INTRODUCTION

Obesity is a complex and multifaceted health disorder that has become a pressing public health challenge of the 21st century. It is associated with poor health outcomes and increased mortality risks. In order to combat the rising obesity rate worldwide, the food industry has a pivotal role in promoting healthier eating habits by reducing the total calorie intake from fat, an energy-dense macronutrient contributing 9 kcal g^{-1}. This is evidenced by the widely available low-calorie, reduced-calorie, and zero-calorie products on market shelves.

Mayonnaise is a versatile and widely used condiment that has a high fat content of 70–80%. As such, low fat and reduced-fat versions of mayonnaise are gradually populating supermarket shelves as a healthier option for consumers. However, when fat content in mayonnaise is reduced, oil droplet density in mayonnaise decreases as well, resulting in the loss of stability, firmness, and viscosity of the mayonnaise (Mirzanajafi-Zanjani et al., 2019). Usually, fat replacers such as protein, carbohydrate, and fat are utilized to reduce the calorie content in mayonnaise (Chang et al., 2017; Li et al., 2014; H. Liu et al., 2007). Nonetheless, carbohydrates like starch and high fructose corn syrup have the potential to increase the risk of diseases such as diabetes and heart diseases. Fat mimetics derived from dietary fiber sources serve as an alternative to conventional fat replacers that confer to health benefits and negate the adverse effects mentioned above.

Nanocellulose is a nanoscaled biopolymer made up of β-1,4 linked D-glucoanhydropyranose. It has a diameter usually in the range of 5–40 nm and length of 100–500 nm, which can be produced from a range of cellulosic materials (Endes et al., 2016). Owing to the many desirable properties of nanocellulose such as biocompatibility, viscosifying properties, zero-calorie properties, chemical inertness, and amphiphilic nature, nanocellulose has attracted great interest among researchers as a green, renewable, and sustainable raw material for food applications (Serpa et al., 2016). This is in accordance with the current food trend where sustainable development is part of the core focus area. One of the most distinctive features of nanocellulose, especially cellulose nanofibers (CNF) is its viscosifying properties. Entanglement of cellulose fibers gives rise to a stable three-dimensional gel network which is able to act as a rheological modifier in reduced fat food products. The use of CNF in combination with other food additives such as starch and guar gum in low-fat mayonnaise formulation has shown improved organoleptic properties with high stability during storage (Golchoobi et al., 2016; Heggset et al., 2020). According to US Food and Drug Administration (FDA) regulations, nutrient comparative claim can be done when a product has reduced nutrient content of at least 25% compared to its reference food (Wartella et al., 2011). To the best of our knowledge, the use of CNF alone in reducing mayonnaise fat content up to 30% has yet to be studied, thus posing an interesting research gap in the current literature to investigate its ability to act as rheological modifier in reduced fat mayonnaise. Besides, several mechanisms have also been proposed by past researches in regard to the putative health benefits of nanocellulose, especially on its antiobesity effect. For example, CNF can lower lipolysis rate by hindering access of lipase to lipid droplets and binding to bile salt in the body (Bai et al., 2019; DeLoid et al., 2018; Liu & Kong, 2019). Furthermore, the nanosized cellulose acts as a prebiotic in the gut which boosts production of short chain fatty acid and alters the gut microbiome (Nsor-Atindana et al., 2020).

In light of the growing trend towards the use of sustainable raw materials in food products, this study aims to study the effect of incorporating CNF synthesized from palm pressed fiber (PPF), an underutilized oil palm biomass in Malaysia, as a rheological modifier and fat mimetic in reduced fat mayonnaise. The physicochemical properties of reduced fat mayonnaise (5%, 10%, and 30%) and its storage stability over a period of 20 days were evaluated. Additionally, this study examined the antiobesity effect of CNF via in silico molecular docking between CNF and human pancreatic lipase (HPL).

2 | MATERIALS AND METHODS

2.1 | Materials

Palm kernel olein oil (PKOO) and PPF were supplied by Sime Darby Research Plantation Sdn Bhd (Pulau Carey, Malaysia), while 1,3 specific Lipozyme TLIM lipase were purchased from Novozymes A/S (Bagsvaerd, Denmark). Flaxseed oil (FO), soybean oil, egg yolk, vinegar, sugar, and salt were sourced from the local supermarkets. FO and soybean oil were used to produce medium and long chain triacylglyceride (MLCT), a type of antiobesity functional oil, using the optimized reaction conditions obtained in a previous study conducted by Lee et al. (2015). Substrate ratio of PKOO and FO (90:10 w/w) were interesterified with 5% of TLIM at 50°C for 7.26 h. Upon completion of reaction, the synthesized oil was filtered to separate enzyme lipase from oil and acidified using 15% NaOH solution at 1:20 (w/w) NaOH to oil ratio to eliminate free fatty acid. The final free fatty acid content achieved was 0.035%, which was below 0.1% according to the standard set by The Palm Oil Refiners Association of Malaysia(2000). Subsequent high-performance liquid chromatography analysis revealed a total yield of 71.24% MLCT triglyceride formed after interesterification reaction. All chemicals

and reactants used in this research were of analytical grade.

2.2 | Synthesis of palm-based CNFs

2.2.1 | Cleaning of PPF

Before use, big substances like stones, seeds, and leaves were removed from PPF by handpicking. PPF were then soaked in distilled water for 3 h, followed by rinsing with hot water (60°C) to remove dirt adhering to the fiber surface. After washing, the PPF were dried overnight in an oven at 60°C. The dried PPF were then grounded using a PX-MFC90D lab mill (Polymix, Switzerland) with a 2-mm sieve attachment and sifted with a 60-mesh sieve. Ground PPF were then stored at 4°C until further use.

2.2.2 | Alkali and bleaching treatments

Firstly, ground PPF were soaked in 4% NaOH at a fiber to solution ratio of 1 g:15 ml at room temperature for 2 h. Next, the ground PPF were heated in 17.5% NaOH at 80°C with stirring at a fiber to solution ratio of 1 g:15 ml for 4 h. The alkali-treated fibers (AT-PPF) were filtered and washed with distilled water to remove excess alkali until neutral pH was obtained.

Peracetic acid solution was prepared beforehand by combining glacial acetic acid and 30% hydrogen peroxide solution at a ratio of 6:4 (in ml) followed by 1.5% of sulfuric acid. The solution was then stirred at room temperature for 72 h before use. After alkali treatment, bleaching treatment was conducted by adding AT-PPF to 80°C peracetic acid solution at a fiber to solution ratio of 1 g:20 ml for 1 h. The bleaching treatment was conducted twice. The bleached fiber were then stirred in 1.0 M NaOH for 1 h (1 g:20 ml) to neutralize the peracetic acid. Finally, distilled water was used to wash the alkali-treated and bleached fibers (AB-PPF) until pH of neutrality was reached.

Extraction of CNFs

The pretreated cellulose were dispersed in distilled water at a concentration of 1% and passed through PandaPLUS 2000 High Pressure Homogenizer (HPH) (GEA Group, Düsseldorf, Germany). The cellulose slurry were passed through HPH under different pressures at 30 MPa, 50 MPa, and 70 MPa for one cycle which were labeled as CNF-30, CNF-50, and CNF-70 respectively. Samples from CNF-70 were further subjected to different cycles of HPH treatment. Cycles 2, 3, and 4 of HPH treatment at 70 MPa correspond to CNF-70(2), CNF-70(3), and CNF(4), respectively. The CNF were then stored at 4°C until further use.

2.3 | Characterization of CNFs

2.3.1 | Color measurement

Color of raw PPF and AB-PPF was analyzed using color spectrophotometer (Colorflex EZ, Hunterlab, Melbourne, Australia) following the $L*$, $a*$, $b*$ system to evaluate color changes in the fiber after chemical pretreatments.

2.3.2 | Zeta potential

Zeta potential of 0.05% CNF dispersed in distilled water were measured using Malvern Nano-ZS Zetasizer (Malvern Instruments Ltd, Worcestershire, UK) at room temperature (25°C) using electrophoretic light scattering method.

2.3.3 | Rheology measurement

Rheology properties of CNF were measured using a MCR 302 modular compact rheometer (Anton Paar, Graz, Austria) with a parallel plate (50 mm diameter and 1 mm gap) at 25°C. The viscosity of CNF samples were analyzed by varying the shear rate from 0.01 s^{-1} to 300 s^{-1}. The flow curve obtained were then analyzed using the Hershel-Bulkley model:

$$\sigma = \sigma_0 + K\gamma^n \quad (1)$$

where σ = shear stress (Pa), σ_0 = yield stress (Pa), γ = shear rate (s^{-1}), K = consistency coefficient (Pa s^n), n = flow behavior index.

2.3.4 | Fourier transform infrared spectroscopy

Fourier transform infrared (FTIR) spectra of raw PPF, AT-PPF, AB-PPF, and CNF-70(2) were analyzed using an infrared Fourier-transform spectrometer (Perkin Elmer Spectrum Two, Perkin Elmer, Waltham, MA, USA) to examine changes in functional groups during CNF production. The FTIR spectra analyses were performed at a resolution of 4 cm^{-1} in the infrared region of 400–4000 cm^{-1} with a total of 16 scans for each sample.

2.3.5 | Field electron scanning electron microscope

Prior to viewing under field electron scanning electron microscope (FE-SEM), the samples were first fixed on a

carbon-filled tape and coated with gold at a sputtering current of 30 mA, sputter time of 38 s and tooling factor of 1.10 using a rotary pumped coater (Quorum Q150R S, Quorum Technologies, Lewes, UK). The morphology and diameter of freeze-dried raw PPF, AB-PPF, and CNF-70(2) were examined using FE-SEM (Hitachi SU8010, Tokyo, Japan) at 10 kV accelerating voltage under magnifications of 100×, 500×, and 1000×. ImageJ software was used to measure the diameter of raw PPF, AB-PPF, and CNF-70(2).

2.4 | Preparation of mayonnaise

Mayonnaise were formulated based on the formulation in Table 1. Egg yolk, vinegar, water, sugar, salt, and CNF-70(2) were blended using an ultra Turax homogenizer (IKA T25, Staufen, Germany) at 350 rpm for 5 min. Soybean oil and MLCT were then added in a dropwise manner to the aqueous phase while increasing the speed of homogenizer to 550 rpm for 10 min. Mayonnaise samples were placed in a tube and stored at 25°C for 20 days. Samples were collected at day 1, 10, and 20 for analysis.

2.4.1 | Characterization of mayonnaise

Rheology analysis
Viscoelastic property of the mayonnaise samples were evaluated using a MCR 302 modular compact rheometer (Anton Paar, Graz, Austria) attached with a 50-mm parallel plate with 1-mm gap at 25°C. The linear viscoelastic region (LVR) of each sample was determined using strain sweep oscillatory test with strain ranging from 0.01% to 100% at a fixed frequency of 1 Hz. Subsequently, frequency sweep test ranging from 0.01 Hz to 100 Hz were performed at 1% strain, which was within the LVR region of the mayonnaise samples. The components of storage modulus (G′), loss modulus (G″), and tan δ versus frequency of all mayonnaise samples were obtained.

Micromorphology of mayonnaise
Mayonnaise samples were spread thinly on a microscope slide and covered with a cover slip prior to viewing under light microscope (Olympus BX51, Tokyo, Japan) at a magnification of 400× to observe the morphology and size of oil droplets.

Color measurement
Color of mayonnaises were inspected using a color spectrophotometer (Colorflex EZ, Hunterlab, Melbourne, Australia) following the L^*, a^*, b^* system.

$$\Delta E = \sqrt{\left(\Delta L^*\right)^2 + \left(\Delta a^*\right)^2 + \left(\Delta b^*\right)^2} \qquad (2)$$

TABLE 1 Formulation of full fat and reduced fat 5%, 15%, and 30% mayonnaise

Ingredients (%)	Full fat	Reduced fat 5% (RF5)			Reduced fat 15% (RF15)			Reduced fat 30% (RF30)		
		M1	M2	M3	M1	M2	M3	M1	M2	M3
Soybean oil	42	37	37	37	27	27	27	12	12	12
MLCT	28	28	28	28	28	28	28	28	28	28
Egg yolk	18	18	18	18	18	18	18	18	18	18
Vinegar	8	8	8	8	8	8	8	8	8	8
Sugar	2	2	2	2	2	2	2	2	2	2
Salt	2	2	2	2	2	2	2	2	2	2
CNF	–	0.001	0.005	0.033	0.05	0.1	0.15	0.2	0.25	0.3
Water	–	4.999	4.995	4.967	14.95	14.9	14.85	29.8	29.75	29.7
Total	100	100	100	100	100	100	100	100	100	100

Abbreviations: CNF, cellulose nanofiber; MLCT, medium- and long-chain triacylglycerol.

Separation/creaming Index

The external appearance of each tube was observed for macroscopic defects such as the occurrence of syneresis and/or emulsion separation during long-term storage. The extent of creaming was evaluated quantitatively by first measuring the height of emulsion (HE) and the height of serum layer (HS). Creaming index was calculated using the formula below:

$$\%CI = (HS/HE) \times 100 \qquad (3)$$

pH measurement

pH of mayonnaise were measured using pH meter (Seven2Go pH meter S2-Std-Kit, Mettler Toledo, OH, USA) at room temperature (25°C).

2.5 | Statistical analysis

Statistical analyses were carried out using IBM SPSS Statistics version 27. Statistical differences between samples were evaluated using analysis of variance (ANOVA) approach followed by post hoc LSD test.

2.6 | Molecular docking

As the antiobesity effect of CNF has been established in several studies, it is of interest to examine and verify the possible interaction between CNF and HPL. The structure of HPL (PDB ID: 1lpb) and orlistat (PubChem CID: 3034010) was downloaded from Protein Data Bank and PubChem. The structure of CNF was constructed and downloaded using an online tool known as Cellulose Builder. The molecular docking procedures were carried out using AutoDock Vina software version 1.1.2. The docking results were visualized and analyzed using Pymol version 2.5.1. and Discovery Studio Visualizer version 4.0.

3 | RESULTS AND DISCUSSION

3.1 | Isolation and characterization of CNFs

3.1.1 | Color analysis

Figure 1a portrays the appearance of raw PPF as brown in color due to the presence of lignin and other chromophore components. After alkaline and bleaching pretreatments, the PPF turned into a white, soft mass as depicted in Figure 1c. The significant change in color may be due to the solubilization of lignin and decomposition of peracetic acid, forming hydrogen peroxide, which reacts with

the chromophoric portion of PPF through chemisorptions (Dungani et al., 2017). The color changes of PPF were further measured quantitatively using color spectrophotometer, and the results are shown in Table 2. The *L** value, representing the lightness of the sample, increased significantly after chemical pretreatments. This is attributed to the bleaching effect of peracetic acid that enhances the brightness and whiteness of PPF by removing dark colored tannins and lignin

3.1.2 | Zeta potential

Zeta potential measures the magnitude of negative charge on nanocellulose surface that confers to colloidal stability due to same charge electronic repulsion. In this study, as HPH pressure increases from 30 MPa to 70 MPa, absolute zeta potential of CNF increases from -44.1 ± 1.37 mV to -57.7 ± 1.82 mV. These results are related to HPH processing that fibrillates cellulose via a shearing action. As a result, more hydroxyl groups in cellulose were exposed, increasing the negative charge on CNF surface. Besides, oxidation of functional groups on CNF surface takes place due to increased contact between CNF and oxygen, thus increasing the absolute zeta potential value of CNF (Ni et al., 2020). This finding was consistent with the study by Ni et al. (2020) who reported increment in absolute zeta potential value from -41.4 mV to -52.6 mV with increasing HPH pressure (10 MPa to 70 MPa). By increasing the number of cycles of HPH processing, cellulose fibers were further fibrillated as shown by the significant increase in absolute zeta potential value from -57.7 ± 1.82 mV to -72.5 ± 2.26 mV after two rounds of HPH treatment at 70 MPa. Contrary to expectations, absolute zeta potential value decreased at three and four cycles of HPH treatment, which could be due to the re-agglomeration of CNF fibers. As the fibers re-agglomerate together, less negatively charged functional groups will be exposed on the fiber aggregate surface, thus reducing the zeta potential measured. This justification was supported by Lenhart et al. (2020) who reported that increasing number of HPH cycle beyond the optimum energy needed for cellulose fibrillation could cause re-agglomeration of CNF due to increase in exposed hydroxyl groups on CNF surface and the subsequent hydrogen bonding between functional groups. The re-agglomeration of CNF decreases the magnitude of negative charge on CNF surface, thus lowering its ability to confer to colloidal stability (Table 3).

3.1.3 | Rheology

CNF exhibits a gel-like behavior after HPH processing due to the entanglement of thin, long cellulose fibrils that
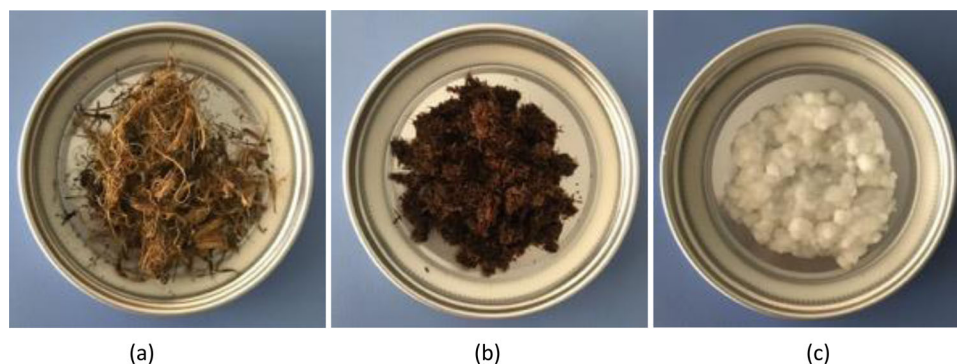
FIGURE 1 Images of (a) raw PPF, (b) AT-PPF, (c) AB-PPF
Abbreviations: AB-PPF, alkali-treated and bleached palm pressed fiber; AT-PPF, alkali-treated palm pressed fiber; PPF, palm pressed fiber

TABLE 2 Color coordinates and color changes of raw PPF and AB-PPF

Colour coordinates	L^*	a^*	b^*	$\triangle E$
Raw PPF	28.50 ± 0.01^a	6.10 ± 0.02^a	15.42 ± 0.05^a	49.20 ± 0.02
AB-PPF	74.16 ± 0.00^b	-0.90 ± 0.00^b	-1.50 ± 0.02^b	

Note: Results are expressed mean $\pm$ standard deviation of triplicate analysis. Different superscript alphabets in the same column indicate a significant difference at $p < 0.05$.
Abbreviations: AB-PPF, alkali-treated and bleached palm pressed fiber; PPF, palm pressed fiber.

TABLE 3 Zeta potential measurement of AB-PPF and CNF

Samples			Zeta potential (mV)
AB-PPF			-37.2 ± 5.08^a
CNF	Pressure (MPa)	Number of cycles	
CNF-30	30	1	-44.1 ± 1.37^b
CNF-50	50	1	-43.4 ± 0.06^b
CNF-70	70	1	-57.7 ± 1.82^{cA}
CNF-70(2)	70	2	-72.5 ± 2.26^B
CNF-70(3)	70	3	-46.9 ± 1.97^C
CNF-70(4)	70	4	-51.95 ± 5.44^{AC}

Note: Zeta potential is expressed as the mean $\pm$ standard deviation of triplicate measurements of each sample. Different lowercase superscript alphabets indicate a significant difference between samples at different pressure at $p < 0.05$. Different uppercase letter superscripts indicate a significant difference between samples at different number of cycles at $p < 0.05$.
Abbreviations: AB-PPF, alkali-treated and bleached palm pressed fiber; CNF-30, CNF treated at 30 MPa; CNF-50, CNF treated at 50 MPa; CNF-70, CNF treated at 70 MPa; CNF-70(2), CNF treated at 70 MPa for two cycles; CNF-70(3), CNF treated at 70 MPa for three cycles; CNF-70(4), CNF treated at 70 MPa for four cycles.

forms a fiber network. The shear flow properties of CNF under different HPH conditions in this study are shown in Figure 2. Shear stress of all the CNF samples increased with shear rate, indicating that CNF exhibits a shear thinning behavior. Figure 2 also shows a stepwise increment

in viscosity of CNF as homogenization pressure increases from 30 MPa to 70 MPa. Higher homogenization pressure applied on the cellulose slurry causes degree of cellulose fibrillation to increase, thus reducing cellulose particle size and increasing the aspect ratio of CNF. By increasing the aspect ratio of CNF, the number of fibril contact points rises, entrapping more water within the gel network and shifting the rheology of the cellulose slurry to a more viscous and gel-like behavior (Ang et al., 2019; Moberg et al., 2017). Increasing number of homogenization cycle at 70 MPa to two cycles further increased the viscosity of CNF. This was in line with the work by Lenhart et al. (2020) who observed formation of a more viscous CNF gel during each additional homogenization cycle. Contrary to expectation, no observable changes in CNF viscosity were spotted when homogenization cycle increases to three and four cycles which can be attributed to the re-agglomeration of cellulose fibers.

3.1.4 | FE-SEM

Figure 3a,b depicts the surface morphology of raw PPF which was rough with irregularly shaped pits on the surface due to presence impurities and macromolecules such as wax, pectin, lignin, hemicellulose, and fatty substances. As can be seen in Figure 3c,d, the surface of AB-PPF is smoother and cleaner with no observable pits. Besides,
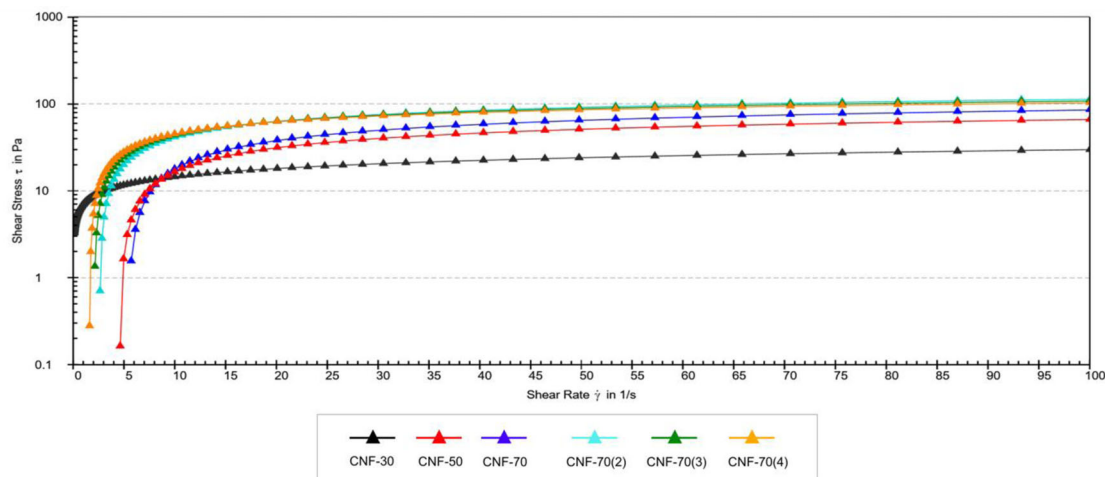
FIGURE 2 Flow curve of shear stress versus shear rate of CNF under varying HPH conditions

Abbreviations: CNF-30, CNF treated at 30 MPa; CNF-50, CNF treated at 50 MPa; CNF-70, CNF treated at 70 MPa; CNF-70(2), CNF treated at 70 MPa for two cycles; CNF-70(3), CNF treated at 70 MPa for three cycles; CNF-70(4), CNF treated at 70 MPa for four cycles

thin fibril structures in parallel with the fiber axis can be observed after chemical pretreatments. The drastic change in the surface morphology is ascribed to the dissolution of noncellulosic materials on fiber surface from the combined action of NaOH and peracetic acid (Ho et al., 2011). Besides changes in surface morphology, the fibers experienced significant size reduction from 188.4 μm ± 5.6 μm to 5.87 μm ± 1.4 μm ($p < 0.05$) after chemical pretreatments. Subsequent HPH treatment at 70 MPa for two cycles was used to delaminate fiber fragments via high pressure, shear, turbulence, and cavitation (Nagarajan et al., 2021). This led to the physical unwinding of native cellulose fibers, producing a heterogeneous mixture of thin cellulose fibers with different diameters that are highly entangled as shown in Figure 3e,f. The approximate diameter of CNF-70(2) measured using ImageJ was 106.0 ± 18.7 nm.

3.1.5 | FTIR

Changes in fiber functional groups at different stages of CNF production are shown in Figure 4 and Table 4. In the FTIR spectra of raw PPF, the peak at 2850 cm^{-1} represents C = O functional group in fatty acid molecule, indicating the presence of residual oil on fiber surface. Following alkali treatment, the peak at 2850 cm^{-1} disappeared which shows that residual oil on PPF surface was successfully removed. Attenuation of absorption peak at 2918 cm^{-1}, corresponding to the symmetric and asymmetric stretching of lignocellulosic aliphatic–CH groups, and the disappearance of the peak at 1709 cm^{-1}, corresponding to the C = O carbonyl functional groups in hemicellulose and lignin, following alkali treatment implied the removal of small amounts of lignocellulosic material, which is consistent

with the findings reported by Chieng et al. (2017). The peak shift at 2918 cm^{-1} to 2892 cm^{-1} and disappearance of peaks ranging from 1500 cm^{-1} to 1630 cm^{-1} corresponding to the C = H bond in aromatic ring and C–H vibration in lignin in AB-PPF illustrate the effective removal of lignin in PPF during bleaching process. It is also noted that the peak at 895 cm^{-1}, representing the anomeric vibration specific to beta glucosidic linkage between sugar units, was not evident in raw PPF but was present in AT-PPF, AB-PPF, and CNF. This may due to the presence of hemicellulose, lignin, and other noncellulosic components that encrusts cellulose in raw PPF (Shanmugarajah et al., 2015). After bleaching process, two new peaks emerged in the FTIR spectra of AB-PPF which are the peaks at 1427 cm^{-1} and 1159 cm^{-1}, corresponding to –CH group and C–O–C groups in cellulose, respectively. From these results, it can be suggested that the removal of noncellulosic material from PPF helps expose more cellulose functional groups. After HPH treatment, new peaks formation at 1637 cm^{-1} and 1107 cm^{-1} that corresponds to water absorption by cellulose molecule and C–O stretch in secondary alcohol, respectively, as well as increase in intensity in both peak at 1637 cm^{-1} and 1313 cm^{-1} (O–H bend in phenol or tertiary alcohol) were observed. These results can be related to the fibrillation action of HPH treatment that led to increase in exposed –OH groups on fibril surface and water absorption by CNF (Freitas et al., 2015; Shanmugarajah et al., 2015).

3.2 | Characterization of mayonnaise

Considering the relatively high zeta potential and viscosity of CNF produced at 70 MPa and two cycles as compared to

TABLE 4 Assignment and intensity of specific infrared absorption peak of raw PPF, AT-PPF, AB-PPF, and CNF-70(2)

Wavenumber (cm⁻¹)	Assignment	Relative intensity of peaks			
		Raw PPF	AT-PPF	AB-PPF	CNF-70(2)
3330	O–H group (primary and secondary alcohol) in cellulose	Moderate	Moderate	Moderate	Moderate
2917	Alipathic –CH symmetric and asymmetric stretching	Strong	Low	Low	Low
2850	C = O in fatty acid	Strong	No peak	No peak	No peak
1709	C = O group in acetyl and ester from hemicellulose and phenolic acid	Moderate	No peak	No peak	No peak
1637	Water absorption by cellulose molecule	No peak	No peak	Low	Moderate
1626	C = H in aromatic ring and C–H vibration in lignin	Moderate	No peak	No peak	No peak
1591		Low	Moderate	No peak	No peak
1504		Low	Moderate	No peak	No peak
1427	C-H group in cellulose	No peak	No peak	Low	Moderate
1319	C–H vibration in cellulose and C–O vibration in lignin	Very low	Low	Low	Moderate
1243	=C-O group in lignin	Moderate	Low	No peak	No peak
1159	C–O–C vibration in cellulose and hemicellulose	No peak	No peak	Strong	Strong
1030	–C–O stretching in cellulose and hemicellulose	Strong	Strong	Strong	Strong
895	Anomeric vibration specific to beta glucosidic linkage between sugar units	No peak	Moderate	Strong	Strong

Abbreviations: AB-PPF, alkali-treated and bleached palm pressed fiber; CNF-70(2), CNF treated at 70 MPa for two cycles; PPF, palm pressed fiber.
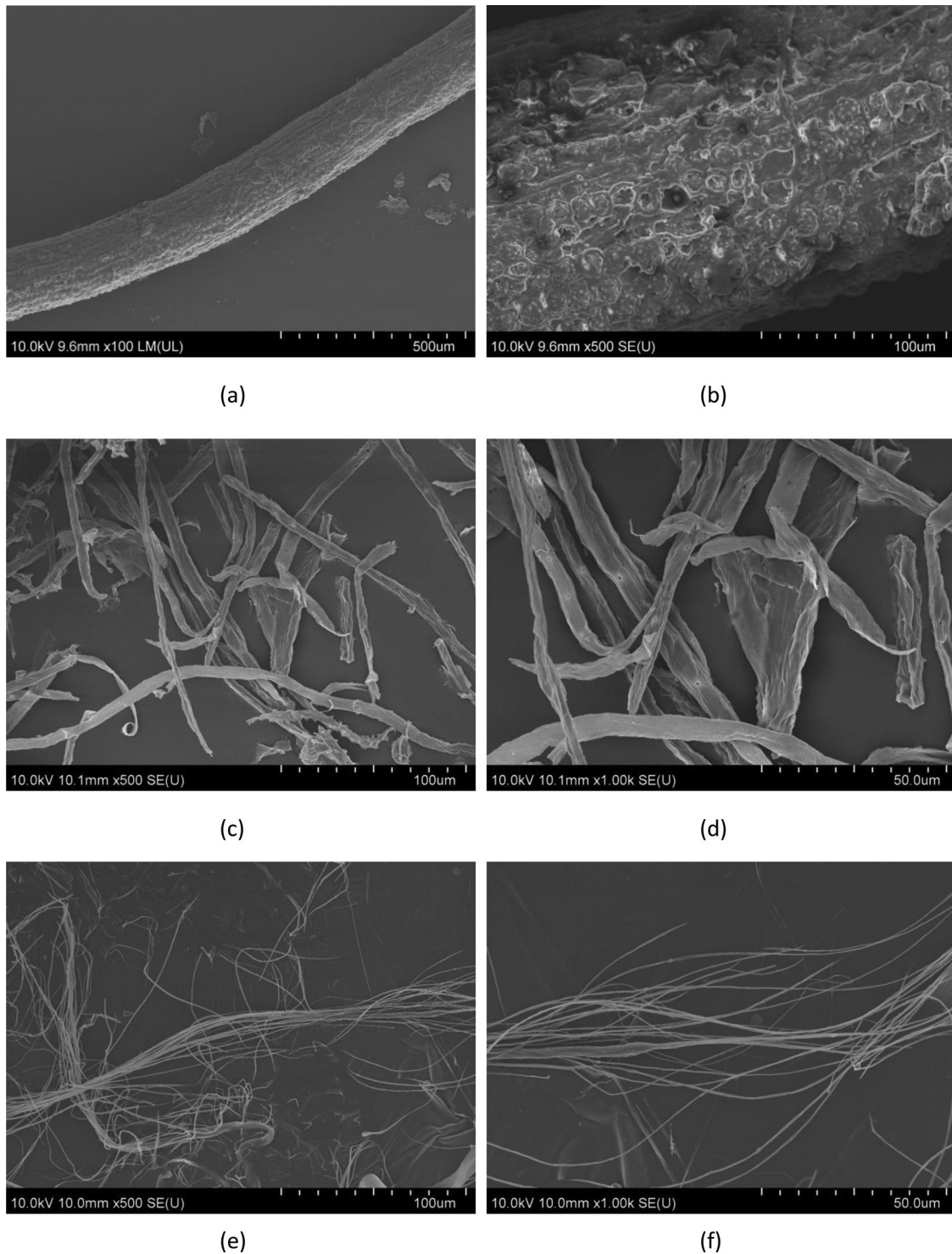
FIGURE 3 FE-SEM images of raw PPF (a and b), AB-PPF (c and d) and CNF-70(2) (e and f) at magnification of 100×, 500× and 1000× Abbreviations: AB-PPF, alkali-treated and bleached palm pressed fiber; CNF-70(2), CNF treated at 70 MPa for two cycles; PPF, palm pressed fiber

the other counterparts, this CNF is regarded to be an ideal candidate to act as a fat mimetic and emulsion stabilizer in food system. Henceforth, the emulsion-stabilizing effect of this CNF in a reduced-calorie mayonnaise was investigated in the subsequent study.

3.2.1 | Rheology analysis

The viscoelastic behavior of mayonnaise samples were measured and the storage modulus (G′) and loss modulus (G″) of each sample are presented in Figure 5–7. From
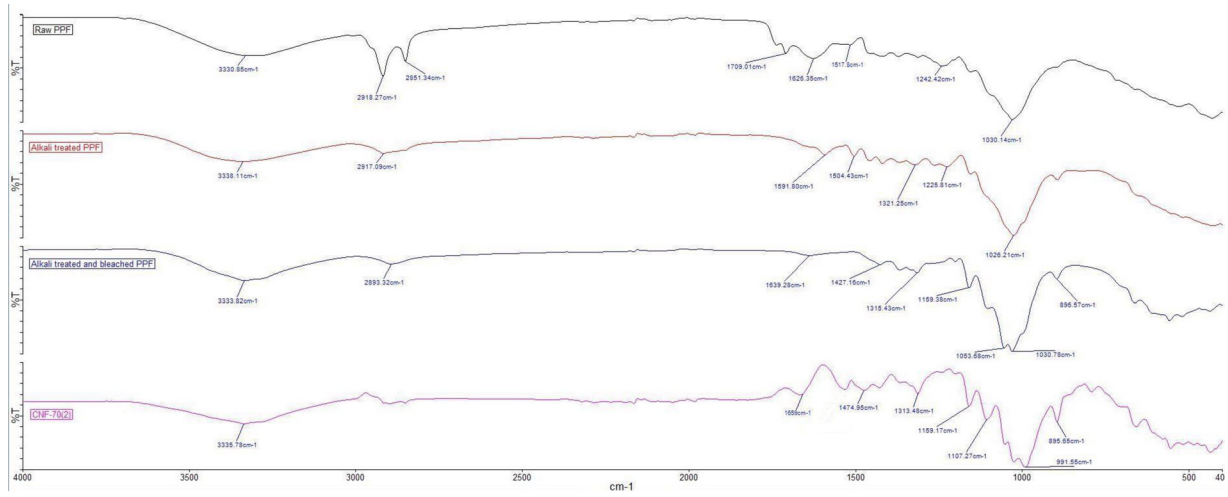
Figure 1. FTIR spectra of raw PPF, AT-PPF, AB-PPF and CNF-70(2). PPF = palm pressed fiber; AB-PPF = alkali-treated and bleached palm pressed fiber; CNF-70(2) = CNF treated at 70 MPa for 2 cycles.

FIGURE 4 FTIR spectra of raw PPF, AT-PPF, AB-PPF, and CNF-70(2)
Abbreviations: AB-PPF, alkali-treated and bleached palm pressed fiber; CNF-70(2), CNF treated at 70 MPa for two cycles; PPF, palm pressed fiber
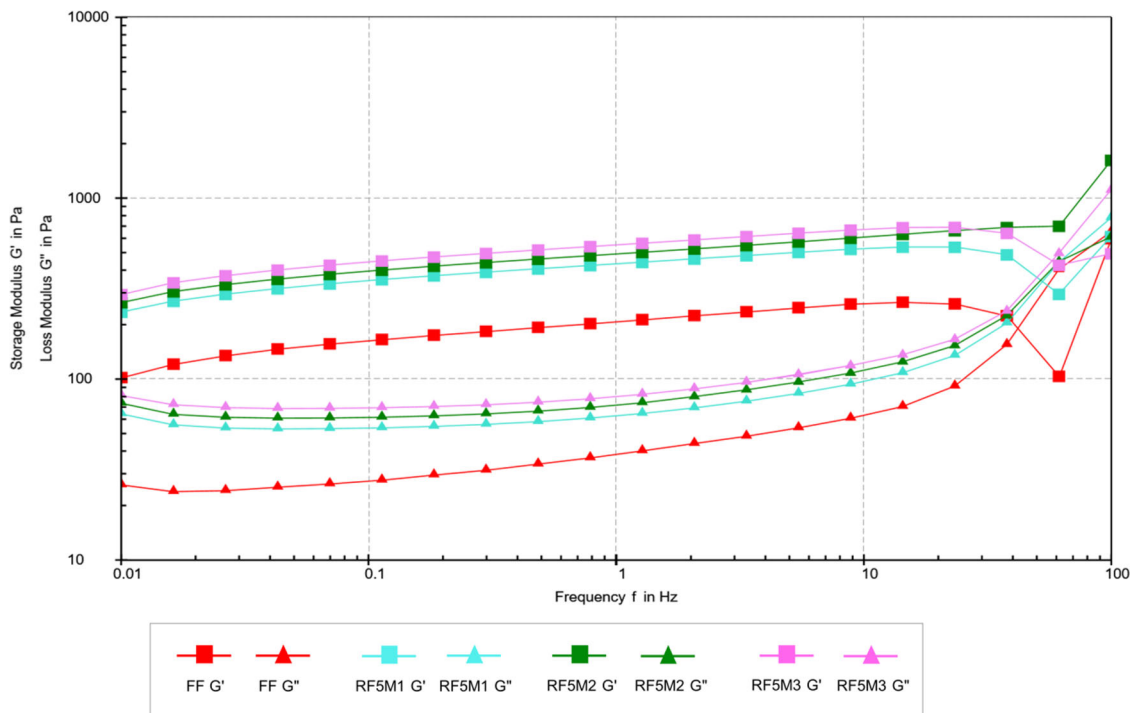
FIGURE 5 Graph of storage modulus (G′) indicated by square markers and loss modulus (G″ indicated by triangle markers versus frequency of full fat (FF) and reduced fat 5% (RF5) mayonnaise
Abbreviations: FF, full fat; RF5M1, reduced fat 5% formulation 1; RF5M2, reduced fat 5% formulation 2; RF5M3, reduced fat 5% formulation 3

Figure 5–7, it can be observed that the G′ value of all samples are higher than G″ values (G′ > G″). This shows that the mayonnaise samples have an elastically dominant characteristic over viscous characteristic which is consistent with previous studies (Carcelli et al., 2020; Phuah et al., 2016).

In our study, all reduced fat mayonnaise samples except RF30M1 and RF30M2 had a higher G′ value than full fat mayonnaise despite their lower fat content (Figure 5–7). The greater fat level reduction in RF30 caused an increment of water content in mayonnaise which led to reduced firmness and viscosity. Hence, a higher concentration of
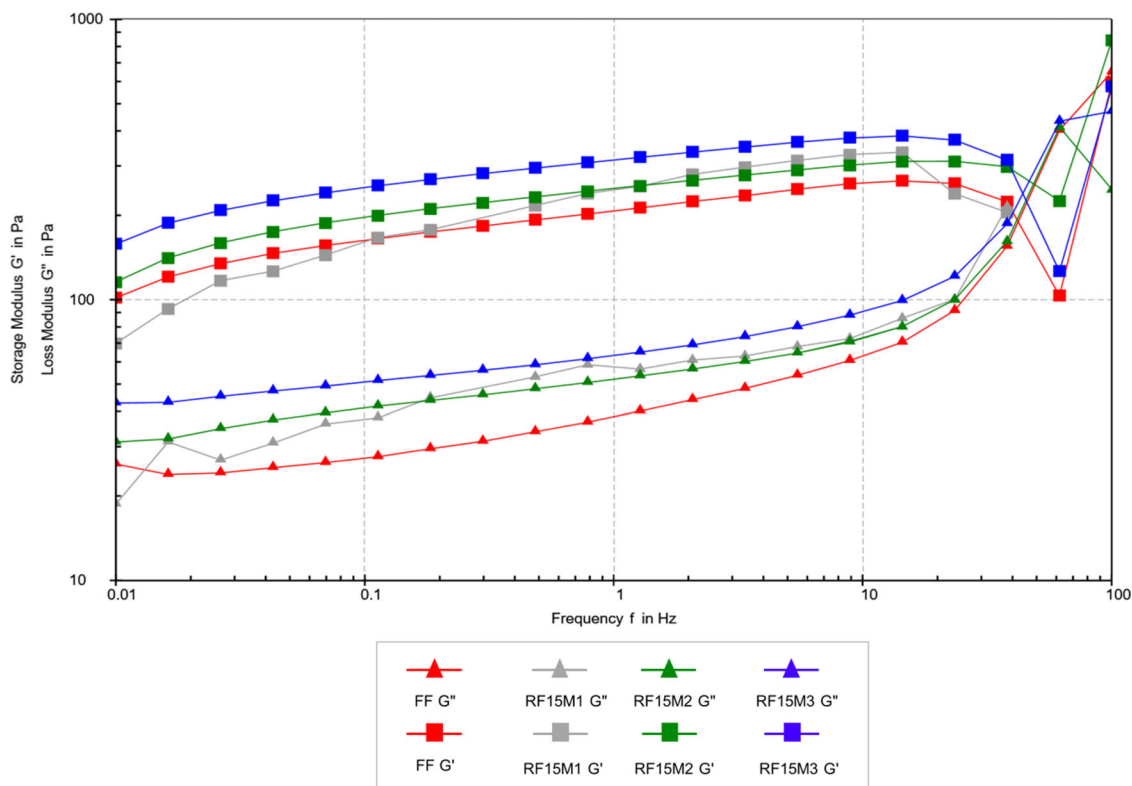
FIGURE 6 Graph of storage modulus (G′) indicated by square markers and loss modulus (G″) indicated by triangle markers versus frequency of full fat (FF) and reduced fat 15% (RF15) mayonnaise
Abbreviations: FF, full fat; RF15M1, reduced fat 15% formulation 1; RF15M2, reduced fat 15% formulation 2; RF15M3, reduced fat 15% formulation 3

CNF at 0.3% was required to mitigate the loss of rheological property in mayonnaise. Nonetheless, the results of this study reflect the ability of CNF to form a 3D gel network in the continuous phase of mayonnaise which helps to compensate for the loss of viscosity caused by reduction in mayonnaise fat content. This is supported by the microstructure analysis of mayonnaise that revealed smaller oil droplet size which are tightly packed in reduced fat mayonnaise samples (except RF30M1 and RF30M2) as compared to full fat mayonnaise (Table 6). Compact packing of oil droplets confers to the elastic behavior and deformation resistance in mayonnaise, resulting in the higher G′ value observed (H. Liu et al., 2007). These results are in agreement with previous research that reported restoration of viscosity and moduli in reduced fat mayonnaise with the incorporation of food additives such as CNF and modified starch (Carcelli et al., 2020; Heggset et al., 2020). In addition, the incorporation of CNF which has a high number of –OH groups exposed may induce the formation of various molecular interactions with protein and fat within the food matrix which confers to the formation of a strong gel network.

3.2.2 | Emulsion stability and microstructure

Food emulsions are thermodynamically unstable food system that have tendency towards coalescence, flocculation, and creaming, leading to the separation of oil and aqueous phase. Creaming index of all mayonnaise samples were 0.00% over the 20 days of storage at room temperature, indicating high emulsion stability. Visual assessment of the mayonnaise samples on day 1, 10, and 20 of storage also revealed no signs of macroscopic defects such as syneresis or oil separation (Table 5). These results were within our expectations which could be due to the high emulsification property of egg yolk that helps maintain emulsion stability.

Droplet microstructures of the formulated mayonnaise were observed under a light microscope and are shown in Table 6. Microscopic appearance of full fat mayonnaise revealed closely packed spherical oil droplets that are relatively uniform in size surrounded by the continuous aqueous phase. The oil droplet particle sizes in RF5 and RF15 samples were smaller compared with FF and some of the oil droplets in RF5 and RF15 samples lost their sphericity and adopted a distorted shape due to close packing of
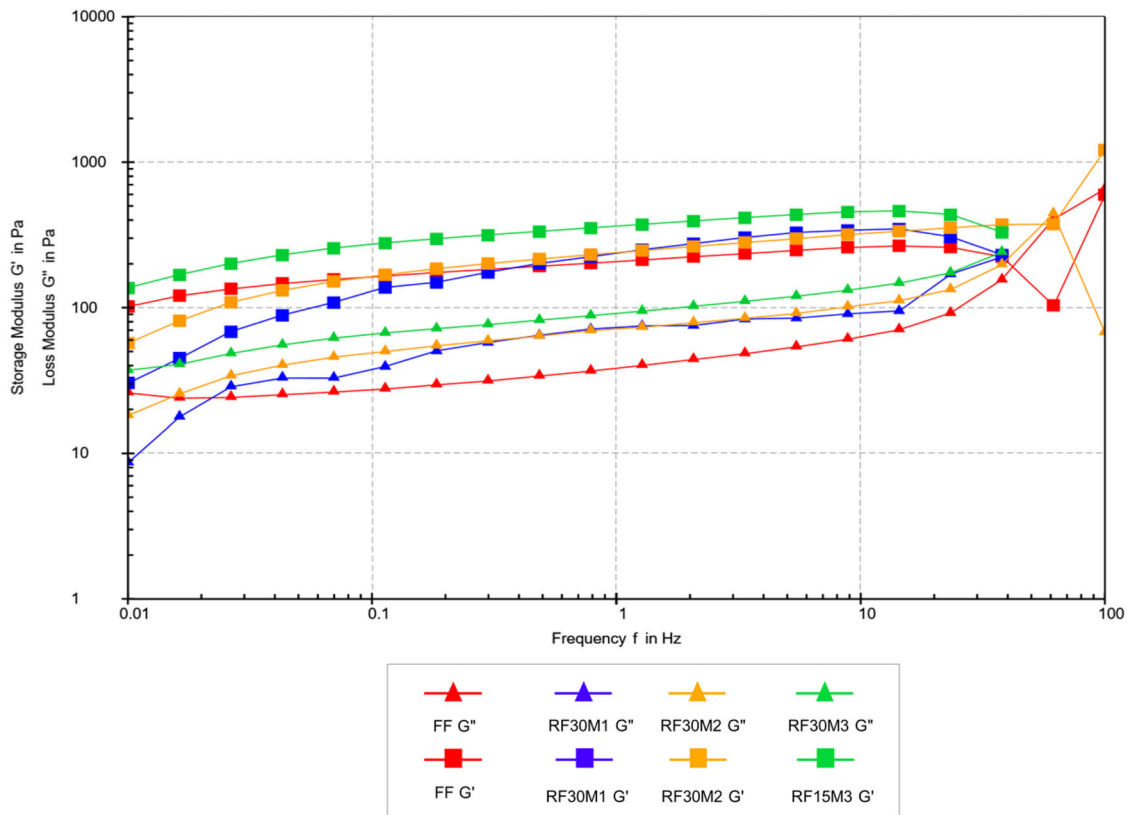
FIGURE 7 Graph of storage modulus (G′) indicated by square markers and loss modulus (G″) indicated by triangle markers versus frequency of full fat (FF) and reduced fat 30% (RF30) mayonnaise

Abbreviations: FF, full fat; RF30M1, reduced fat 30% formulation 1; RF30M2, reduced fat 30% formulation 2; RF30M3, reduced fat 30% formulation 3

the oil droplets. It can also be observed that the decrease in oil droplet size was most prominent in RF5M3 and RF15M3 due to higher concentration of CNF added.

A trend of decreasing oil particle size can also be clearly observed with increasing CNF concentration for all reduced fat mayonnaise formulations. This phenomenon is due to the higher concentration of CNF added that contributes to the formation of a more rigid and closely-packed gel network with smaller pore formations that entraps the oil droplets. Besides, as CNF causes increased viscosity of the continuous aqueous phase in mayonnaise, this decreases the Brownian motion and collision between oil droplets, hence reducing the size of oil droplets. The smaller oil droplet size gives rise to the higher viscosity of mayonnaise as small oil droplets have a bigger surface area that generates a higher frictional force, restricting free flowing of the sample (Phuah et al., 2016). These results are consistent with the rheological analysis discussed above that showed G′ and G″ value increasing with the addition of CNF.
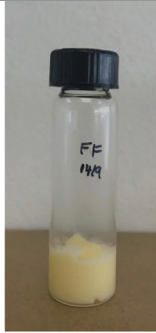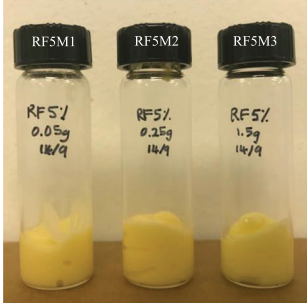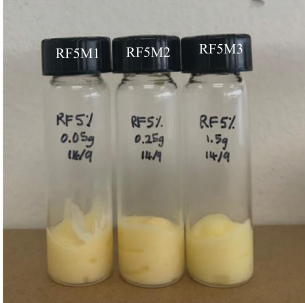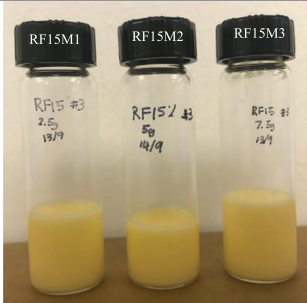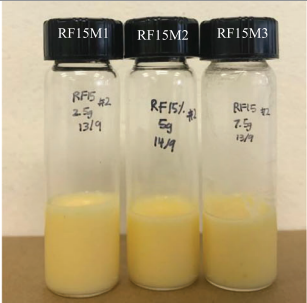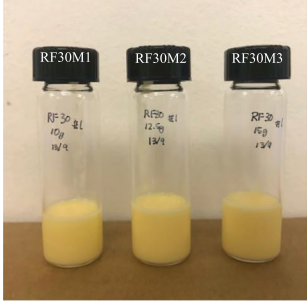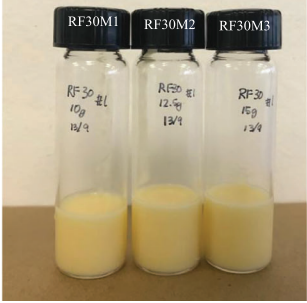
However, when fat content in mayonnaise was reduced by 30%, microstructure of the mayonnaise showed larger oil droplets than the full fat mayonnaise. In 30% RF mayonnaise, more water is added into the formulation,

leading to a less viscous emulsion formed. This increases Brownian motion and collision between oil droplets, leading to oil droplet coalescence. Larger oil droplets formed could lead to emulsion instability and decreased viscosity. For mayonnaise formulations with higher concentration of CNF added (all formulations except RF5M1 and RF5M2), streaks of CNF can be observed in the micrograph of mayonnaise which is similar to the results reported by Carcelli et al. (2020) that used modified corn flour gel as fat replacer in reduced fat mayonnaise formulation.

Although macrophotos of mayonnaise indicated emulsion stability, significant changes in microstructure of mayonnaise were observed throughout the 20-day storage period. As mayonnaise age, the size distribution of oil droplets will change, producing larger oil droplets over time due to Brownian motion, and coalescence of oil droplets (Ariizumi et al., 2017). Consistent with the literature, this study found that oil droplet size increased in tandem with storage period for all mayonnaise samples (Table 6). One unanticipated finding was that the increase in oil droplet size was larger in reduced fat mayonnaise samples with CNF added as compared to full fat mayonnaise. Previous studies have reported that oil droplet

TABLE 5 Creaming index of mayonnaise samples on day 1, day 10, and day 20 storage at 25°C

Samples	Day 1	Day 10	Day 20
FF			
RF5 M1 RF5 M2 RF5 M3			
RF15 M1 RF15 M2 RF15 M3			
RF30 M1 RF30 M2 RF30 M3			

Note: Results are expressed mean ± standard deviation of triplicate analysis.
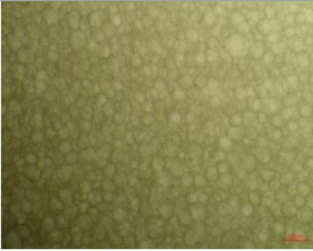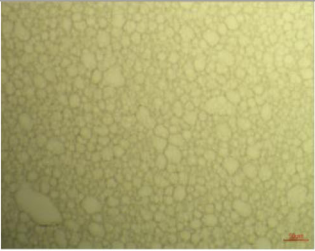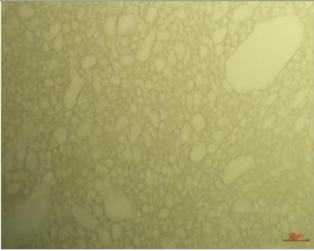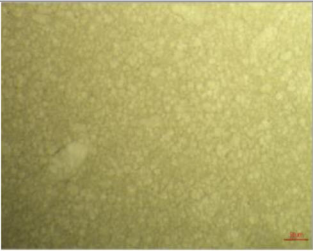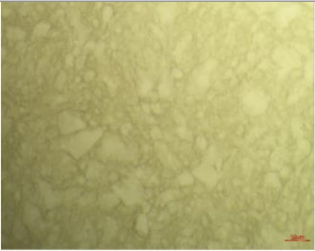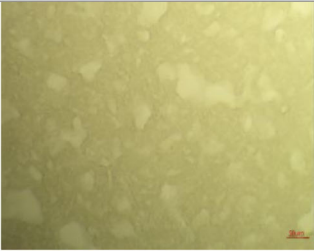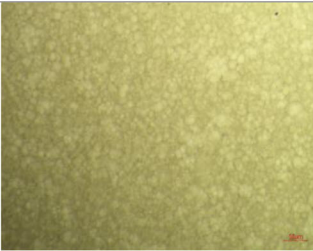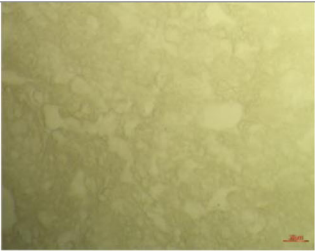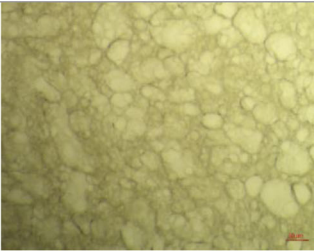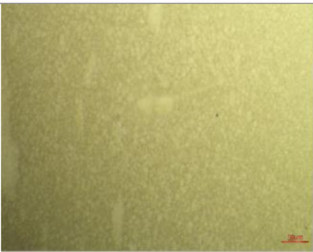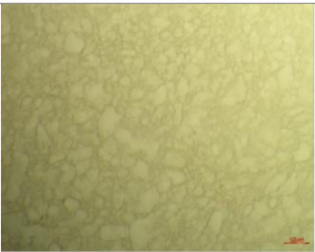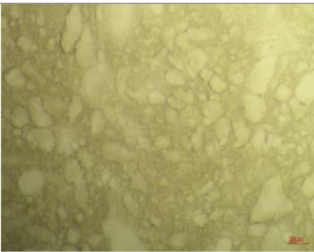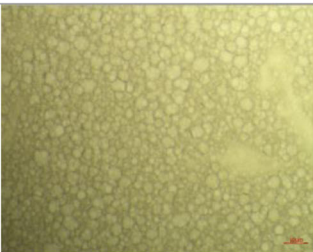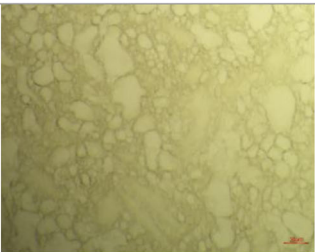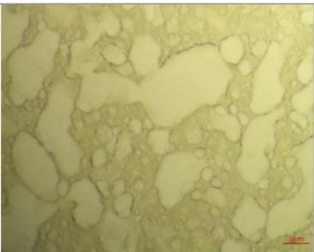
Abbreviations: FF, full fat; RF5M1, reduced fat 5% formulation 1; RF5M2, reduced fat 5% formulation 2; RF5M3, reduced fat 5% formulation 3; RF15M1, reduced fat 15% formulation 1; RF15M2, reduced fat 15% formulation 2; RF15M3, reduced fat 15% formulation 3; RF30M1, reduced fat 30% formulation 1; RF30M2, reduced fat 30% formulation 2; RF30M3, reduced fat 30% formulation 3.

movement in reduced fat products are usually restricted by the addition of thickening agent (Carcelli et al., 2020). The results in this study may be due to the decrease in pH on day 10 (Table 8). Reduction in pH led to the increased in protonation of carboxyl groups on CNF, further enhancing interfibril interaction via the dimerization of carboxyl groups. This results in the formation of dense gels of CNF

in the aqueous phase that are segregated from the bulk liquid, thus causing the loss of gel formation in the aqueous phase that encapsulates the oil droplets. This justification is supported by L. Liu et al. (2018) that observed separation of nanocellulose gel from bulk liquid under low pH condition. Consequently, viscosity of the aqueous phase decreases, leading to the increased Brownian motion
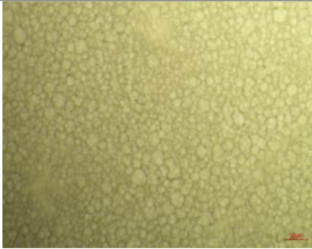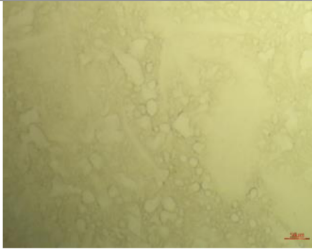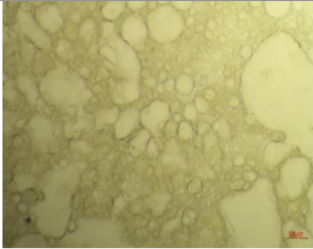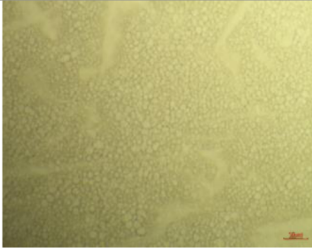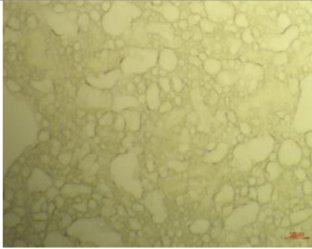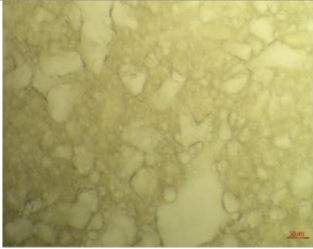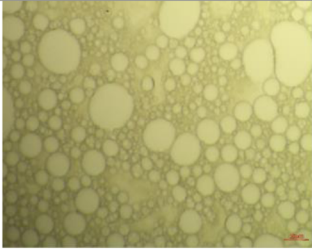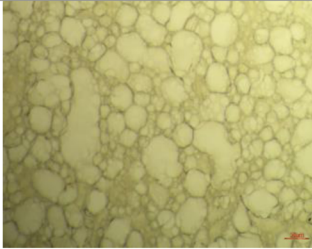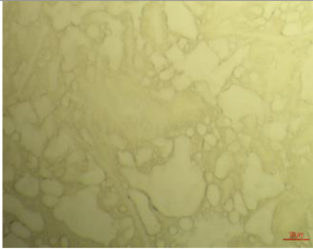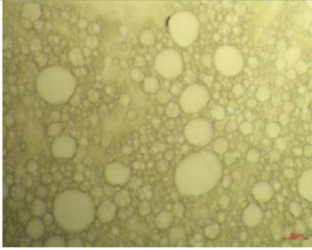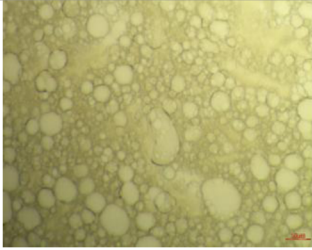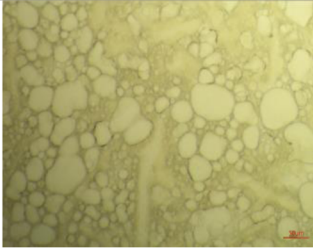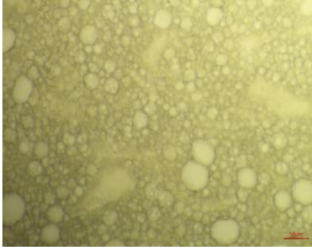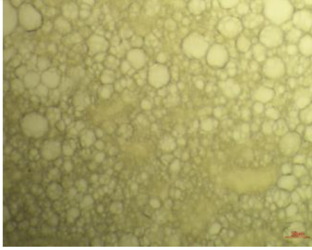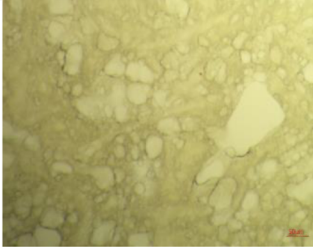
TABLE 6   Visual assessment of mayonnaise on day 1, day 10, and day 20 storage at 25°C

Samples	Day 1	Day 10	Day 20
FF			
RF5 M1			
RF5 M2			
RF5 M3			
RF15 M1			

(Continues)

TABLE 6 (Continued)

Samples	Day 1	Day 10	Day 20
RF15 M2			
RF15 M3			
RF30 M1			
RF30 M2			
RF30 M3			

Abbreviations: FF, full fat; RF5M1, reduced fat 5% formulation 1; RF5M2, reduced fat 5% formulation 2; RF5M3, reduced fat 5% formulation 3; RF15M1, reduced fat 15% formulation 1; RF15M2, reduced fat 15% formulation 2; RF15M3, reduced fat 15% formulation 3; RF30M1, reduced fat 30% formulation 1; RF30M2, reduced fat 30% formulation 2; RF30M3, reduced fat 30% formulation 3.

TABLE 7 Colour parameters and colour changes (ΔE) in mayonnaise on day 1, day 10 and day 20 storage at 25°C

	Day	FF	RF5 M1	RF5 M2	RF5 M3	RF15 M1	RF15 M2	RF15 M3	RF30 M1	RF30 M2	RF30 M3
L*	0	81.34 ± 0.55[abA]	81.57 ± 0.98[aceA]	81.20 ± 0.39[abA]	82.12 ± 0.54[aeA]	80.40 ± 0.75[bA]	81.21 ± 0.17[abA]	81.33 ± 0.54[bcdA]	80.54 ± 0.76[bcA]	81.89 ± 0.23[adeA]	82.51 ± 0.56[eA]
	10	80.27 ± 0.15[B]	81.11 ± 0.59[A]	81.18 ± 0.31[A]	81.89 ± 0.50[A]	81.21 ± 0.16[A]	81.56 ± 0.30[A]	81.24 ± 0.22[A]	82.14 ± 0.66[AB]	83.04 ± 0.46[AB]	83.07 ± 0.33[AB]
	20	80.30 ± 0.14[B]	79.05 ± 0.92[B]	79.87 ± 0.28[B]	80.41 ± 0.21[B]	80.35 ± 0.94[A]	79.98 ± 0.81[B]	80.16 ± 0.64[A]	83.36 ± 0.54[B]	83.49 ± 0.66[B]	83.67 ± 0.32[B]
a*	0	7.21 ± 0.08[aA]	7.29 ± 0.18[aA]	7.25 ± 0.21[aA]	7.17 ± 0.22[aA]	6.15 ± 0.95[bA]	6.87 ± 0.36[abA]	6.04 ± 0.25[bA]	6.65 ± 0.58[abA]	6.58 ± 0.70[abA]	6.45 ± 0.66[abA]
	10	6.49 ± 0.26[B]	6.68 ± 0.28[A]	6.56 ± 0.29[A]	6.04 ± 0.83[B]	4.91 ± 0.76[A]	5.89 ± 0.14[B]	5.80 ± 0.38[A]	5.72 ± 0.37[B]	5.94 ± 0.29[A]	5.77 ± 0.18[A]
	20	4.57 ± 0.32[C]	4.09 ± 0.69[B]	3.68 ± 1.00[B]	3.25 ± 0.32[C]	2.41 ± 0.42[B]	3.93 ± 0.65[C]	2.97 ± 0.37[B]	3.46 ± 0.27[C]	2.95 ± 0.17[B]	3.50 ± 0.30[B]
b*	0	36.76 ± 0.54[abA]	37.37 ± 0.84[aA]	37.19 ± 0.74[acA]	36.55 ± 0.55[abA]	37.24 ± 0.26[abA]	36.73 ± 0.95[abA]	35.48 ± 0.76[bcdA]	37.03 ± 0.36[abA]	36.19 ± 0.73[bdA]	34.20 ± 0.89[dA]
	10	37.80 ± 0.42[A]	35.81 ± 0.97[AB]	36.40 ± 0.61[AB]	35.50 ± 0.86[AB]	33.15 ± 0.76[B]	34.48 ± 0.42[AB]	33.43 ± 0.88[B]	32.75 ± 0.69[B]	32.18 ± 0.85[B]	31.92 ± 0.29[B]
b*	20	35.40 ± 0.43[A]	34.09 ± 0.46[B]	34.56 ± 0.86[B]	33.66 ± 1.30[B]	29.83 ± 1.01[C]	32.34 ± 1.72[B]	30.16 ± 0.70[C]	28.27 ± 1.14[C]	27.39 ± 0.73[C]	28.10 ± 0.74[C]
ΔE	0	—	—	—	—	—	—	—	—	—	—
	10	1.66 ± 0.74	1.82 ± 0.41	1.22 ± 0.12	1.95 ± 0.25	3.50 ± 1.01	2.50 ± 0.93	2.21 ± 1.65	4.11 ± 0.23	3.56 ± 0.96	2.56 ± 0.82
	20	3.12 ± 0.41	5.31 ± 0.53	4.70 ± 1.30	5.20 ± 0.86	7.48 ± 2.47	5.61 ± 1.86	6.19 ± 1.25	9.16 ± 0.39	8.95 ± 0.81	6.91 ± 0.90

a,b Different letter superscripts in the same row indicate a significant difference at $p < 0.05$ between different mayonnaise samples.

A,B Different letter superscripts in the same column indicate a significant difference at $p < 0.05$ of the same sample throughout the storage period.

Results are expressed in mean ± standard deviation of triplicate analysis. FF = full fat; RF5M1 = reduced fat 5% formulation 1; RF5M2 = reduced fat 5% formulation 2; RF5M3 = reduced fat 5% formulation 3; RF15M1 = reduced fat 15% formulation 1; RF15M2 = reduced fat 15% formulation 2; RF15M3 = reduced fat 15% formulation 3; RF30M1 = reduced fat 30% formulation 1; RF30M2 = reduced fat 30% formulation 2; RF30M3 = reduced fat 30% formulation 3.

of oil droplets and further promoting the occurrence of coalescence.

3.2.3 | Color

Color of mayonnaise originates from egg yolk and oil, with carotenoids present in egg yolk being the primary source of the distinct yellow color of mayonnaise. The color of all mayonnaise samples are shown in Table 7. In our study, a small increase in L^* value can be observed as the concentration of CNF increases for each reduced fat mayonnaise formulation, with the most significant change observed in RF30M3. This may be ascribed to the light scattering ability of CNF that shifts the color paradigm of emulsion from grey to white (Golchoobi et al., 2016). A significant lowering of a^* value (redness) was observed in RF15 and RF30 mayonnaise which can be related to reduced oil content and increased lightness of mayonnaise, causing colors in mayonnaise to fade. The b^* value (yellowness) of all reduced fat mayonnaise samples were insignificantly different from FF except RF30M2 and RF30M3 samples. This could be due to the greater reduction in fat content coupled with higher CNF concentration added that causes color of RF30M2 and RF30M3 to be paler.

During the 20-day storage period, decrease in a^* and b^* values were observed in all samples, whereas L^* value decreased in all samples except in RF30 samples. In accordance with the present results, previous studies have reported that decrease in L^* value was ascribed to the increase in oil particle size during long-term storage of mayonnaise (Ghorbani Gorji et al., 2019). Significant decrease in both a^* and b^* value reflects changes in mayonnaise color which could be due to oxidative decomposition of different ingredients in mayonnaise, especially oil. The incorporation of omega-3-enriched MLCT further aggravates the autoxidation process as polyunsaturated fatty acids are more susceptible to radical attacks as compared to saturated fatty acids. Besides oxidation of oil, carotenoids present in egg yolk may oxidize and degrade as they contain large number of double bonds. This is justified by a study that reported a correlation between loss of α- and β-carotene with decrement in b^* value (Lennersten & Lingnert, 2000). The change in color in mayonnaise samples were further supported by ΔE values. It can be seen from the data in Table 7 that ΔE values exceeded 5.0 on day 20 of storage, indicating that the color change was more prominent and may affect consumer's sensory acceptability.

3.2.4 | pH

From a microbiological standpoint, mayonnaise made with unpasteurized egg yolk should have a pH of 4.1 or below to control *Salmonella* growth. As can be seen in

TABLE 8 pH of mayonnaise samples on day 1, 10, and 20 storage at 25°C

Samples	pH		
	Day 1	Day 10	Day 20
FF	2.43 ± 0.03	2.51 ± 0.05	3.64 ± 0.06
RF5 M1	2.28 ± 0.05	2.33 ± 0.03	3.40 ± 0.20
RF5 M2	2.29 ± 0.01	2.28 ± 0.04	3.50 ± 0.03
RF5 M3	2.24 ± 0.04	2.28 ± 0.03	3.41 ± 0.06
RF15 M1	2.32 ± 0.02	1.96 ± 0.05	3.58 ± 0.03
RF15 M2	2.36 ± 0.06	1.88 ± 0.12	3.54 ± 0.06
RF15 M3	2.36 ± 0.06	2.02 ± 0.27	3.52 ± 0.06
RF30 M1	2.35 ± 0.02	2.11 ± 0.02	3.53 ± 0.08
RF30 M2	2.42 ± 0.05	2.26 ± 0.05	3.53 ± 0.06
RF30 M3	2.36 ± 0.02	2.39 ± 0.04	3.55 ± 0.02

Note: Results are expressed mean ± standard deviation of triplicate analysis.
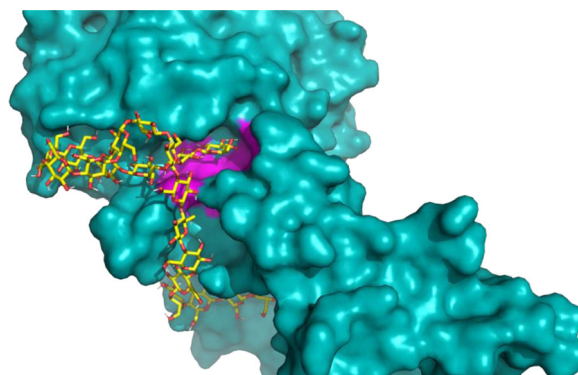
FIGURE 8 Docking position of CNF (yellow) in active site of HPL (pink)

Table 8, the pH of mayonnaise samples in this study are below 4.1, thus ensuring microbial safety of mayonnaise. It can also be observed that the pH of reduced fat mayonnaises were lower than full fat mayonnaise. This may be ascribed to the residual peracetic acid present in CNF that causes the lowering of pH in mayonnaise. In this study, the pH of mayonnaises were found to be lower than the literature value that ranges between 3.51 and 4.25 (Kishk & Elsheshetawy, 2013; Naznin et al., 2010). This may be due to the higher amount of vinegar added to the formulation and the residual FFA present in the synthesized MLCT oil. The lower pH of mayonnaise formulated in this study could promote gelling property of CNF. Pääkkö et al. (2007) and Ni et al. (2020) reported increment in shear viscosity of CNF at lower pH due to neutralization of negative charge by hydrogen ions ($COO^- + H^+ \rightarrow COOH$) which in turn enhances interfibrillar interaction between cellulose fibrils.

After storage of 10 days, the pH of all mayonnaise samples decreased slightly. Autoxidation of double bonds in unsaturated fatty acid esters and hydrolysis of the

TABLE 9 Binding affinity and interaction of orlistat, acarbose, and CNF with HPL and HPA

Protein	Compound	Binding affinity (kcalmol^{-1})	Interaction with amino acids		
			Hydrogen bonding	Hydrophobic interaction	Attractive charge
Human pancreatic lipase (HPL)	Orlistat	−7.5	His151, Ser152, Leu153	Phe216, Ile78, Leu264, Arg256	His263
	CNF	−5.8	His151, Arg256, His263, Asn189, Asp79, Asn212, Asn229, Phe77, Asn212, Ala259, Glu233	–	–

Abbreviation: CNF, cellulose nanofibers.

acylglycerols may take place in the presence of water in mayonnaise and atmospheric oxygen in the headspace of mayonnaise, leading to the formation of FFA (Abu-Salem & Abou-Arab, 2008). This was shown in the study by Chukwu and Sadiq (2008) that recorded increase in FFA content from 0.73% to 2.40% in mayonnaise throughout 6 weeks of storage. The increase in FFA content results in the initial decrease of pH as observed in this study. Surprisingly, increase in mayonnaise pH were observed after 20 days of storage but the pH values were still below 4.1, which means that the mayonnaise were still safe from a microbiological aspect. This result is at odds with previous studies that reported stable pH or decrease in pH during long-term storage of mayonnaise (Heggset et al., 2020; Triawati et al., 2016). Interestingly, Choublab and Winuprasith (2018) that utilized CNF as emulsifier in the formulation of egg yolk-free mayonnaise also reported a significant increment in pH after 6–8 weeks of storage. A possible explanation for this result is the formation of strong hydrogen bonds between CNF fibers over time that led to formation of heterogeneous clumps of fibers in the aqueous phase. This may lead to the expulsion of water initially trapped within the CNF gel network, thus causing increase in amount of free water present in mayonnaise and the subsequent dilution of acetic acid.

3.3 | Molecular docking

3.3.1 | Human pancreatic lipase

Human pancreatic lipase (HPL) consisting of key amino acids Ser152, Phe215, Arg256, His263, and Leu264 present in the duodenum is responsible for 50–70% of lipolysis of triglycerides in the body (Vu et al., 2017). Ser152 plays a vital role in hydrolyzing ester bonds during lipolysis of fats and oil (Vu et al., 2017). Orlistat showed strong binding to HPL with the formation of six hydrogen bonds at His151, Ser152, and Leu153, among which four hydrogen bonds were formed with Ser152 (Table 9). Besides hydro-

gen bonding, orlistat also interacts with amino acids in HPL via hydrophobic interaction and attractive charges. Al-Suwailem et al. (2006) stated that orlistat forms a stable complex with lipase by binding covalently to its active site and inducing conformational changes in lipase which subsequently leads to the inactivation of lipase. Nonetheless, intake of orlistat has been associated with adverse side effects such as fatty stools and irregular bowel movements (Al-Suwailem et al., 2006).

The interaction between CNF and HPL were weaker at −5.8 kcal mol^{-1} as compared to interaction between orlistat and HPL at −7.5 kcal mol^{-1}. Furthermore, interaction between CNF and HPL existed only in the form of hydrogen bonding. A total of 11 hydrogen bonds were formed between CNF and HPL, among which two of the hydrogen bonds were interacting with Arg256 and His263. Based on the docking pose of CNF, CNF occupies the catalytic site of HPL (Figure 8), suggesting that CNF can potentially reduce lipolysis reaction by either decreasing the binding of triglycerides to HPL or inducing conformational changes in lipase. However, these results differ from a molecular dynamic simulation study conducted by DeLoid et al. (2018) that reported insignificant and short-lived interactions between CNF and HPL. This rather contrary results may arise from the discrepancy in study design and computational software used.

4 | CONCLUSION

In this study, CNF with diameter of 106.0 ± 18.7 nm and zeta potential of −72.5 ± 2.26 mV was successfully isolated from PPF via a combination of chemical pretreatments involving NaOH and peracetic acid as well as mechanical treatment using HPH at 70 MPa for two cycles. Based on the rheology analysis of reduced fat 5%, 15%, and 30% mayonnaise, CNF is able to counterbalance the loss of viscosity and moduli caused by fat reduction in mayonnaise. Besides, oil droplet size in reduced fat 5% and 15% mayonnaise were smaller as compared to full fat

mayonnaise but not in reduced fat 30% mayonnaise. The 20-day stability study conducted showed that although no observable macroscopic defects were detected in mayonnaise samples, microstructure analysis of mayonnaise found a greater extent of oil droplet coalescence in reduced fat mayonnaise. This finding can be related to the drop in mayonnaise pH at day 10 which causes formation of dense CNF gel that is segregated from bulk liquid, hence reducing viscosity of aqueous phase. To sum up, CNF synthesized in this study was able to exhibit viscosifying effect in mayonnaise upon formulation of mayonnaise. However, significant oil droplet coalescence was observed in reduced fat mayonnaise during storage.

AUTHOR CONTRIBUTIONS
Zu Jia Lee: Conceptualization; Data curation; Formal analysis; Investigation; Methodology; Project administration; Resources; Software; Writing—original draft; Writing—review & editing. Shi-Cheng Tong: Conceptualization; Data curation; Formal analysis; Investigation; Methodology; Resources; Writing—review & editing. Teck-Kim Tang: Conceptualization; Methodology; Project administration; Resources; Validation; Writing—review & editing. Yee Ying Lee: Conceptualization; Project administration; Supervision; Validation; Writing—review & editing.

CONFLICT OF INTEREST
The authors declare no conflicting interests.

ORCID
Shi-Cheng Tong https://orcid.org/0000-0002-9037-0579
Yee-Ying Lee https://orcid.org/0000-0002-4586-5978

REFERENCES
Abu-Salem, F. M., & Abou-Arab, A. A. (2008). Chemical, microbiological and sensory evaluation of mayonnaise prepared from ostrich eggs. *Grasas y aceites*, *59*(4), 352–360. https://doi.org/10.3989/gya.2008.v59.i4.529

Al-Suwailem, A., Al-Tamimi, A., Al-Omar, M., & Al-Suhibani, M. (2006). Safety and mechanism of action of orlistat (tetrahydrolipstatin) as the first local antiobesity drug. *Journal of Applied Sciences Research*, *2*, 205–208.

Ang, S., Haritos, V., & Batchelor, W. (2019). Effect of refining and homogenization on nanocellulose fiber development, sheet strength and energy consumption. *Cellulose*, *26*(8), 4767–4786. https://doi.org/10.1007/s10570-019-02400-5

Ariizumi, M., Kubo, M., Handa, A., Hayakawa, T., Matsumiya, K., & Matsumura, Y. (2017). Influence of processing factors on the stability of model mayonnaise with whole egg during long-term storage. *Bioscience, biotechnology, and biochemistry*, *81*(4), 803–811. https://doi.org/10.1080/09168451.2017.1281725

Bai, L., Lv, S., Xiang, W., Huan, S., McClements, D. J., & Rojas, O. J. (2019). Oil-in-water Pickering emulsions via microfluidization with cellulose nanocrystals: 2. In vitro lipid digestion. *Food Hydrocolloids*, *96*, 709–716. https://doi.org/10.1016/j.foodhyd.2019.04.039

Carcelli, A., Crisafulli, G., Carini, E., & Vittadini, E. (2020). Can a physically modified corn flour be used as fat replacer in a mayonnaise? *European Food Research and Technology*, *246*(12), 2493–2503. https://doi.org/10.1007/s00217-020-03592-y

Chang, C., Li, J., Li, X., Wang, C., Zhou, B., Su, Y., & Yang, Y. (2017). Effect of protein microparticle and pectin on properties of light mayonnaise. *LWT – Food Science and Technology*, *82*, 8–14. https://doi.org/10.1016/j.lwt.2017.04.013

Chieng, B., Lee, S., Ibrahim, N., Then, Y., & Loo, Y. (2017). Isolation and characterization of cellulose nanocrystals from oil palm mesocarp fiber. *Polymers*, *9*(12), 355. https://doi.org/10.3390/polym9080355

Choublab, P., & Winuprasith, T. (2018). Storage stability of mayonnaise using mangosteen nanofibrillated cellulose as a single emulsifier. *Journal of Food Science and Agricultural Technology (JFAT)*, *4*, 59–66.

Chukwu, O., & Sadiq, Y. (2008). Storage stability of groundnut oil and soya oil-based mayonnaise. *Journal of Food Technology*, *6*(5), 217–220.

DeLoid, G. M., Sohal, I. S., Lorente, L. R., Molina, R. M., Pyrgiotakis, G., Stevanovic, A., Zhang, R., McClements, D. J., Geitner, N. K., Bousfield, D. W., Ng, K. W., Loo, S. C. J., Bell, D. C., Brain, J., & Demokritou, P. (2018). Reducing intestinal digestion and absorption of fat using a nature-derived biopolymer: Interference of triglyceride hydrolysis by nanocellulose. *ACS Nano*, *12*(7), 6469–6479. https://doi.org/10.1021/acsnano.8b03074

Dungani, R., Owolabi, A. F., Saurabh, C. K., Abdul Khalil, H. P. S., Tahir, P. M., Hazwan, C. I. C. M., Ajijolakewu, K. A., Masri, M. M., Rosamah, E., & Aditiawati, P. (2017). Preparation and fundamental characterization of cellulose nanocrystal from oil palm fronds biomass. *Journal of Polymers and the Environment*, *25*(3), 692–700. https://doi.org/10.1007/s10924-016-0854-8

Endes, C., Camarero-Espinosa, S., Mueller, S., Foster, E. J., Petri-Fink, A., Rothen-Rutishauser, B., Weder, C., & Clift, M. J. D. (2016). A critical review of the current knowledge regarding the biological impact of nanocellulose. *Journal of Nanobiotechnology*, *14*(1), Article number: 78. https://doi.org/10.1186/s12951-016-0230-9

Freitas, N., Aurélio Pinheiro, J., Silva, P., Saraiva Morais, J. P., Filho, M., Brígida, A., Muniz, C., & Rosa, M. (2015). Development of chlorine-free pulping method to extract cellulose nanocrystals from pressed oil palm mesocarp fibers. *Journal of Biobased Materials and Bioenergy*, *9*, 372. https://doi.org/10.1166/jbmb.2015.1525

Ghorbani Gorji, S., Calingacion, M., Smyth, H. E., & Fitzgerald, M. (2019). Effect of natural antioxidants on lipid oxidation in mayonnaise compared with BHA, the industry standard. *Metabolomics*, *15*(8), Article number: 106. https://doi.org/10.1007/s11306-019-1568-4

Golchoobi, L., Alimi, M., Shokoohi, S., & Yousefi, H. (2016). Interaction between nanofibrillated cellulose with guar gum and carboxy methyl cellulose in low-fat mayonnaise. *Journal of Texture Studies*, *47*(5), 403–412.

Heggset, E. B., Aaen, R., Veslum, T., Henriksson, M., Simon, S., & Syverud, K. (2020). Cellulose nanofibrils as rheology modifier in mayonnaise—A pilot scale demonstration. *Food Hydrocolloids*, *108*, 106084.

Ho, T. T. T., Zimmermann, T., Hauret, R., & Caseri, W. (2011). Preparation and characterization of cationic nanofibrillated cellulose from etherification and high-shear disintegration processes. *Cellulose*, *18*, 1391–1406.

Kishk, Y. F., & Elsheshetawy, H. (2013). Effect of ginger powder on the mayonnaise oxidative stability, rheological measurements, and sensory characteristics. *Annals of Agricultural Sciences*, *58*, 213–220. https://doi.org/10.1016/j.aoas.2013.07.016

Lee, Y.-Y., Tang, T.-K., Phuah, E.-T., Ab Karim, N. A., Alwi, S. M. M., & Lai, O.-M. (2015). Palm-based medium-and-long-chain triacylglycerol (P-MLCT): Production via enzymatic interesterification and optimization using response surface methodology (RSM). *Journal of Food Science and Technology*, *52*(2), 685–696. https://www.ncbi.nlm.nih.gov/pmc/articles/PMC4325014/pdf/13197_2013_Article_1065.pdf

Lenhart, V., Quodbach, J., & Kleinebudde, P. (2020). Fibrillated cellulose via high pressure homogenization: Analysis and application for orodispersible films. *AAPS PharmSciTech*, *21*(1), https://doi.org/10.1208/s12249-019-1593-7

Lennersten, M., & Lingnert, H. (2000). Influence of wavelength and packaging material on lipid oxidation and colour changes in low-fat mayonnaise. *LWT – Food Science and Technology*, *33*(4), 253–260. https://doi.org/10.1006/fstl.2000.0660

Li, J., Wang, Y., Jin, W., Zhou, B., & Li, B. (2014). Application of micronized konjac gel for fat analogue in mayonnaise. *Food Hydrocolloids*, *35*, 375–382. https://doi.org/10.1016/j.foodhyd.2013.06.010

Liu, H., Xu, X. M., & Guo, S. D. (2007). Rheological, texture and sensory properties of low-fat mayonnaise with different fat mimetics. *LWT – Food Science and Technology*, *40*(6), 946–954. https://doi.org/10.1016/j.lwt.2006.11.007

Liu, L., Kerr, W. L., Kong, F., Dee, D. R., & Lin, M. (2018). Influence of nano-fibrillated cellulose (NFC) on starch digestion and glucose absorption. *Carbohydrate Polymers*, *196*, 146–153.

Liu, L., & Kong, F. (2019). In vitro investigation of the influence of nano-cellulose on starch and milk digestion and mineral adsorption. *International Journal of Biological Macromolecules*, *137*, 1278–1285. https://doi.org/10.1016/j.ijbiomac.2019.06.194

Mirzanajafi-Zanjani, M., Yousefi, M., & Ehsani, A. (2019). Challenges and approaches for production of a healthy and functional mayonnaise sauce. *Food Science & Nutrition*, *7*(8), 2471–2484. https://doi.org/10.1002/fsn3.1132

Moberg, T., Sahlin, K., Yao, K., Geng, S., Westman, G., Zhou, Q., Oksman, K., & Rigdahl, M. (2017). Rheological properties of nanocellulose suspensions: Effects of fibril/particle dimensions and surface characteristics. *Cellulose*, *24*(6), 2499–2510.

Nagarajan, K. J., Ramanujam, N. R., Sanjay, M. R., Siengchin, S., Surya Rajan, B., Sathick Basha, K., Madhu, P., & Raghav, G. R. (2021). A comprehensive review on cellulose nanocrystals and cellulose nanofibers: Pretreatment, preparation, and characterization. *Polymer Composites*, Advance online publication. https://doi.org/10.1002/pc.25929

Naznin, M. T., Maeda, T., & Morita, N. (2010). Stability of E- and Z-ajoene in home-made mayonnaise. *International Journal of Food Properties*, *13*(2), 317–327. https://doi.org/10.1080/10942910802398461

Ni, Y., Li, J., & Fan, L. (2020). Production of nanocellulose with different length from ginkgo seed shells and applications for oil in water Pickering emulsions. *International Journal of Biological Macromolecules*, *149*, 617–626. https://doi.org/10.1016/j.ijbiomac.2020.01.263

Nsor-Atindana, J., Zhou, Y. X., Saqib, M. N., Chen, M., Goff, H. D., Ma, J., & Zhong, F. (2020). Enhancing the prebiotic effect of cellulose biopolymer in the gut by physical structuring via particle size manipulation. *Food Research International*, *131*, 108935.

Pääkkö, M., Ankerfors, M., Kosonen, H., Nykänen, A., Ahola, S., Österberg, M., Ruokolainen, J., Laine, J., Larsson, P. T., Ikkala, O., & Lindström, T. (2007). Enzymatic hydrolysis combined with mechanical shearing and high-pressure homogenization for nanoscale cellulose fibrils and strong gels. *Biomacromolecules*, *8*(6), 1934–1941. https://doi.org/10.1021/bm061215p

Phuah, E. T., Beh, B. K., Lim, C. S. Y., Tang, T. K., Lee, Y. Y., & Lai, O. M. (2016). Rheological properties, textural properties, and storage stability of palm kernel-based diacylglycerol-enriched mayonnaise. *European Journal of Lipid Science and Technology*, *118*(2), 185–194.

Serpa, A., Velásquez-Cock, J., Gañán, P., Castro, C., Vélez, L., & Zuluaga, R. (2016). Vegetable nanocellulose in food science: A review. *Food Hydrocolloids*, *57*, 178–186.

Shanmugarajah, B., Kiew, P. L., Chew, I. M. L., Choong, T. S. Y., & Tan, K. W. (2015). Isolation of nanocrystalline cellulose (NCC) from palm oil empty fruit bunch (EFB): Preliminary result on FTIR and DLS analysis. *Chemical Engineering Transactions*, *45*, 1705–1710.

The Palm Oil Refiners Association of Malaysia. (2000). PORAM standard specifications for processed palm oil. https://poram.org.my/contracts/poram-standard-specifications-for-processed-palm-oil/

Triawati, N. W., Radiati, L. E., Thohari, I., & Manab, A. (2016). Microbiological and physicochemical properties of mayonnaise using biopolymer of whey protein-gelatin-chitosan during storage. *International Journal of Current Microbiology and Applied Sciences*, *5*(7), 191–199.

Vu, T., Vu, D., Truong, V.-D., Nguyen, P., & Dao, T. (2017). Virtual screening, oriented-synthesis and evaluation of lipase inhibitory activity of benzyl amino chalcone derivatives. *MedPharmRes*, *1*, 26–36. https://doi.org/10.32895/UMP.MPR.1.1.26/suffix

Wartella, E., Lichtenstein, A., Yaktine, A., & Nathan, R. (2011). *Front-of-package nutrition rating systems and symbols: Promoting healthier choices*. The Natural Academies Press. http://doi.org/10.17226/13221